Skin permeation of nickel, cobalt and chromium salts in ex vivo human skin, visualized using mass spectrometry imaging

Toxicology in Vitro 76 (2021) 105232

Contents lists available at ScienceDirect

Toxicology in Vitro

journal homepage: www.elsevier.com/locate/toxinvit

Skin permeation of nickel, cobalt and chromium salts in ex vivo human skin, visualized using mass spectrometry imaging

Lina Hagvall [a,b], Masoumeh Dowlatshahi Pour [a], Jiabao Feng [c], Moshtak Karma [a], Yolanda Hedberg [d], Per Malmberg [c,*]

[a] Department of Dermatology and Venereology, Institute of Clinical Sciences, Sahlgrenska Academy, University of Gothenburg, Gothenburg, Sweden
[b] Region Västra Götaland, Sahlgrenska University Hospital, Department of Dermatology and Venereology, Gothenburg, Sweden
[c] Department of Chemistry and Chemical Engineering, Chalmers University of Technology, Gothenburg, Sweden
[d] Dept. of Chemistry, The University of Western Ontario, London, Ontario, Canada and Surface Science Western, The University of Western Ontario, London, Ontario, Canada

ARTICLE INFO

Editor: Dr P Jennings

Keywords:
Skin permeation
Skin sensitizers
Nickel
Chromium
Cobalt
Chemical speciation modelling

ABSTRACT

Skin permeation and distribution of three of the most common skin sensitizers was investigated using a previously developed animal-free exposure method combined with imaging mass spectrometry. Nickel, cobalt, and chromium (III) salts were dissolved in a buffer and exposed to human skin ex vivo, to be analyzed using time of flight secondary ion mass spectrometry (ToF-SIMS). Our findings demonstrate that metal haptens mainly accumulated in the stratum corneum, however all three metal sensitizers could also be detected in the epidermis. Cobalt and chromium (III) species penetrated into the epidermis to a larger extent than nickel species. The degree of penetration into the epidermis is suggested to be affected by the sensitization potency of the metal salts, as well as their speciation, i.e. the amount of the respective metal present in the solution as bioaccessible and solubilised ions. Our method provided permeation profiles in human skin for known sensitizers, on a level of detail that is not possible to achieve by other means. The findings show that the permeation profiles are different, despite these sensitizers being all metal ions and common causes of contact allergy. Studying skin uptake by only considering penetration through the skin might therefore not give accurate results.

1. Introduction

Allergic contact dermatitis is the symptom of T-cell mediated sensitization, i.e., contact allergy. In order to initiate such a sensitization, it is believed that skin sensitizers first need to penetrate the skin barrier through the stratum corneum, reaching into the epidermis where they bind to skin proteins or other macro molecules thus forming antigens distinguishable to dendritic cells(Karlberg et al., 2008). In general, metals, preservatives and fragrance compounds are the most common causes of contact allergy(Diepgen et al., 2016; Lagrelius et al., 2016), and the most frequent causes of contact allergy to metals in the general population are nickel, cobalt and chromium(Thyssen and Menne, 2010). In the case of metals, metal ions constitute the active hapten and skin contact with everyday metal objects releasing sensitizing metal ions, such as nickel or cobalt ions, can cause allergic contact dermatitis in sensitized individuals(Thyssen et al., 2013). Products containing chromium (III) or chromium (VI) compounds, such as leather are known to cause allergic contact dermatitis in chromium sensitized individuals (Hedberg et al., 2018; Hedberg and Liden, 2016). Experimentally, nickel, cobalt and chromium nanoparticles have been shown to dissolve in artificial sweat, producing ions that can penetrate the skin and directly start an immune response(Stefaniak et al., 2014). It is of great interest to study metal ion penetration, distribution, and interaction within the different layers of the skin. This has so far mostly been studied using quantitative methods with practical limitations such as tape stripping or receptor fluid analysis of diffusion cell experiments.

Clinical studies of skin permeation of nickel using tape stripping or biopsies of positive patch test reactions to nickel have detected nickel in the stratum corneum using inductively coupled plasma atomic emission spectroscopy (ICP-AES) or inductively coupled plasma mass spectrometry (ICP-MS) (Hostynek, 2003; Kalimo et al., 1985), however, nickel could not be detected in deeper skin layers due to the limit of detection of the analysis method or in the case of tape stripping, data collection was stopped before reaching the epidermis for ethical reasons. In

* Corresponding author at: Department of Chemistry and Chemical Engineering, Chalmers University of Technology, Kemivägen 10, 412 96 Gothenburg, Sweden.
E-mail address: malmper@chalmers.se (P. Malmberg).

https://doi.org/10.1016/j.tiv.2021.105232
Received 30 April 2021; Received in revised form 16 July 2021; Accepted 3 August 2021
Available online 6 August 2021

horizontally sliced biopsies from patch tested dermatitis patients exposed to potassium dichromate, chromium (VI) could be detected down to 12 slides deep, using atomic absorption spectroscopy (AAS) (Liden and Lundberg, 1979).

Diffusion cells have been used to study skin penetration of metal salts, where the receptor fluid have been analyzed and/or the skin divided using thermal methods, homogenized, and analyzed separately as stratum corneum, epidermis and dermis. Nickel ions were shown to penetrate through isolated human stratum corneum ex vivo to about 1% (Tanojo et al., 2001). Chromium (III) has been detected at the ug/cm^2 level in acid degraded and homogenized epidermis using AAS (Gammelgaard et al., 1992). Chromium (VI) was detected at 10-fold higher levels in epidermis compared to chromium (III) and also detected in the receptor fluid. A more recent study has investigated permeation of chromium (III) and chromium (VI) salts in human skin using diffusion cells and found similar results (Van Lierde et al., 2006). Chromium (III) was chosen in the present study as previous studies have indicated that chromium (III) passes through the skin to a lesser extent than chromium (VI), and has been suggested to be more reactive towards protein (Siegenthaler et al., 1983).

Skin exposure to metals can also occur in the form of nanoparticles, mainly in an occupational setting. Cobalt and nickel nanoparticles have been shown to penetrate human skin in diffusion cells (Crosera et al., 2016; Larese Filon et al., 2013). Analysis using AAS detected nanoparticles of the respective metal in heat separated and homogenized skin layers. Highest amounts were detected in the epidermis, and nanoparticles were found to penetrate more readily into the skin compared to metal powders of larger particle size (Filon et al., 2009).

Despite these efforts to study skin distribution and penetration of metal ion sensitizers, no method presented allows direct visualization of the distribution of the metal ions in skin tissue, nor simultaneous analysis of endogenous compounds in skin as well as the chemicals or elements to which the skin has been exposed. We recently presented a mass spectrometry imaging-based alternative to these methods, providing detailed qualitative data on distribution of metal ions in the skin tissue and colocalization with endogenous compounds (Malmberg et al., 2018). The method is an animal-free approach, as experiments can be performed ex vivo using human skin tissue which otherwise would be discarded, and it can directly map the distribution of metals in tissue exposed in a conventional diffusion cell experiment. The method provided qualitative information on the localization of nickel metal ions in the stratum corneum of the exposed tissue albeit only at micrometer scale resolution.

Recent ToF-SIMS developments now allow the analysis to be performed at nanometer resolution, while maintaining a sufficient mass resolution to separate metal ions from organic ions (Vanbellingen et al., 2015). Since this would allow a more detailed study of metal ion permeation at a cellular level, we applied this new method to further investigate metal ion penetration in human skin ex vivo. The aim of the present study was to map the distribution in human skin ex vivo after exposure to nickel, cobalt and chromium (III) salts using imaging mass spectrometry. First, we investigated the skin distribution of nickel, cobalt, and chromium (III) salts individually then we compared this to a scenario of simultaneous exposure of all three metal salts in combination. In addition, we perform a full speciation analysis to fully understand metal ion solubility and interaction.

2. Materials and methods

2.1. Chemicals

Ammonium formate, nickel (II) sulfate hexahydrate, cobalt (II) chloride hexahydrate and chromium (III) chloride hexahydrate were purchased from Sigma Aldrich (St Louis, MO, USA).

2.2. Skin exposure

Full-thickness human skin was obtained as left-overs from breast reduction surgery at the Dept. of Plastic Surgery, Sahlgrenska University Hospital. The tissue was made anonymous upon collection in agreement with routines approved by the local ethics committee. The skin tissue was trimmed from subcutaneous fat, cut into 2 × 2 cm pieces, mounted on cork sheets, wrapped in aluminium foil and kept in −20 °C until use within 3 months from surgery. Skin samples from one donor were thawed in room temperature for 30 min prior to experiments. The full thickness skin was mounted in vertical (Franz-type) skin diffusion cells (Laboratory Glass Apparatus, Berkley, CA) having an exposed surface area of 1 cm^2. The receptor compartments were filled with ammonium formate buffer (0.15 M, pH 7.4) to allow best possible mass spectrometry compatibility. Diffusion cells were prepared in which each skin tissue section was separately exposed to nickel (II) sulfate hexahydrate (0.15 M), cobalt (II) chloride hexahydrate (0.15 M) and chromium (III) chloride hexahydrate (0.15 M), and a cocktail solution of these three metal substances (0.45 M in total). A sample exposed to ammonium formate buffer solution served as control. The experiment was performed at room temperature (25 °C) with an exposure time of 24 h. Experiments were performed in duplicate. At removal, skin samples were gently rinsed with distilled water.

2.3. Tissue preparation for ToF-SIMS

Immediately after skin exposure, a small tissue section (approx 8 × 8 mm) was collected at the centre of the exposed region from each skin sample and was then frozen in liquid nitrogen. The frozen skin tissue was sectioned vertically in a cryostat to a thickness of 10 µm. Four slices from the middle of the tissue sample were collected and mounted on indium tin oxide covered (ITO) glass slides for ToF-SIMS analysis. One duplicate glass was prepared for each tissue experiment, which means that 40 skin sections on 10 glass slides were made in total from the 5 types of exposures. At least 4 tissue sections per exposure type were stained using standard Haematoxylin and Eosin staining.

2.4. ToF-SIMS analysis

ToF-SIMS analysis was performed using a ToF.SIMS 5 instrument (ION-ToF GmbH, Münster, Germany). Mass spectra in positive ion mode were recorded by using Bi_3^+ primary ions at 25 keV with a pulsed primary ion current of 0.25 pA. Delayed extraction mode was employed to obtain images with high spatial (approx. 400 nm) and high mass resolution (approx. 5000 at *m/z* 369). Multiple images from each section were recorded in areas of approx. 124 × 124 µm to 150 × 150 µm from the skin sections using a raster of 256 × 256-pixel points. All images and mass spectra were processed, recorded, analyzed and evaluated using the software SURFACELAB (version 7.1, ION-TOF). The spectra were internally calibrated to signals of common fragment such as $[C]^+$, $[CH_2]^+$, $[CH_3]^+$, $[C_5H_{15}PNO_4]^+$, $[C_{27}H_{45}]^+$ for the positive ion mode. Five different sections from exposed specimens of nickel (II) sulfate hexahydrate, cobalt (II) chloride hexahydrate, chromium (III) chloride hexahydrate, a mixed solution of these substances and a control (ammonium formate buffer), respectively, were analyzed.

2.5. Chemical speciation modelling

The joint expert speciation system (JESS) software [was] used to model thermodynamically stable species of the metal ions at pH 7.4 in 0.15 M ammonium formate buffer at 25 °C, atmospheric pressure, and in normal dissolved oxygen conditions (pe 5). For calculations containing cobalt, the following JESS species were excluded to avoid a numerical underflow: $Co(NH_3)_5{}^{3+}$·H2O, $Co(NH_3)_5(COOH)^{2+}$, $Co(NH_3)_5Cl(COOH)^+$, and $Co(NH_3)_5Cl_2(COOH)$. For calculations containing cobalt and chromium, the JESS species $HCo(NH_3)_5CrO_4{}^{2+}$ was excluded

additionally. Solid species were included and allowed to precipitate. First, the predominant solids for the single metal salts were determined. Second, these predominant solids and several combined solids were included in the calculations for the cocktail solution: Co_3O_4, $Ni(OH)_2$, CrOOH, $CoCr_2O_4$, and Cr_2NiO_4. The five most predominating species for each metal salt were evaluated.

3. Results and discussion

Exposure to metal ions occurs in many ways and is difficult to standardize in an experimental model. Most methods that determine metal ion penetration in skin are dependent on tape-stripping or the splitting of the skin layers before analysis. Albeit giving quantitative data, these methods by their very nature allow only a rudimentary understanding of the precise localization of the ions of interest in relation to the surrounding cells in the skin. In this study, by using ToF-SIMS imaging, we provide a direct chemical map of distribution pathways of the most common metal sensitizers in different layers of the skin tissue.

The distribution of cobalt, chromium and nickel ions in tissue exposed to each ion individually, is presented in Fig. 1. H&E-stained skin tissue sections show the marked regions selected for ToF-SIMS analysis. The figure shows red/green color overlay maps of signals of cobalt, chromium and nickel ions, respectively, as well as phosphatidylcholine (PC) headgroup. PC is chosen as a marker for skin tissue in general as it is the most abundant cellular membrane lipid species. Altogether, nickel ions were found to be mainly located in the stratum corneum while the distribution of cobalt and chromium ions was more evenly distributed through the stratum corneum and epidermis. In order to explore this, a line scan analysis, showing signal intensity as a function of depth in the tissue was performed.

Fig. 2 show line scan plots from image data analysis of the relative signal intensity of cobalt, chromium, and nickel ions, respectively, as a function of skin depth. The distribution into the skin tissue for cobalt and chromium ions was similar and showed a substantial accumulation in the deeper skin layers, while nickel ions were mostly accumulated in the stratum corneum. The ToF-SIMS images of the distribution of cobalt, chromium and nickel ions constituting the basis of this analysis are presented in supplemental Fig. S1. Line scans from a replicate experiment can be seen in supplemental Fig. S3. Results from a control experiment are presented in Fig. 2d showing no signal from cobalt, chromium, and nickel ions and only noise in the associated line scan. The line scans used are shown in supplemental Fig. S4.

In order to allow a comparison of the skin penetration for the metal salts in combination, skin tissue sections exposed to a cocktail solution of cobalt chloride, chromium chloride and nickel sulfate was subjected to ToF-SIMS analysis. The H&E-stained image shown in Fig. 3a presents an overview of the skin section analyzed. The marked area indicates the 220 × 220 μm region analyzed with ToF-SIMS.. Fig. 3b shows a color overlay image showing the signals of the PC headgroup, cobalt, chromium, and nickel. A high signal intensity of PC was seen in the epidermis, potentially covering the metal signals in this area. While the metal ions were highly localized to the stratum corneum, penetration into the epidermis was also detected. Chromium signals were predominantly seen in the epidermis followed by cobalt signals in green and nickel signals in yellow, respectively. The distribution of each metal ion in the skin tissue exposed to the cocktail is represented in the single ion images of cobalt, chromium and nickel shown in Fig. 3c–e.

Line scan analysis (Fig. 4) showed that the highest signal intensity was detected from chromium ions in stratum corneum followed by cobalt and lastly nickel ions. Although chromium ions showed the strongest signal in the stratum corneum, cobalt was shown to penetrate the deepest into the skin. Again, nickel ions accumulated in the stratum corneum with little penetration further into the skin. The signal intensities were generally weaker than in the experiments using the metal salts separately. No signals from cobalt, chromium or nickel were detected in the control sample (Fig. 2d and Supplemental Fig. S2).

The bioaccessbility of cobalt, chromium (III) and nickel ions in formate buffer under the conditions of this study was investigated using chemical speciation calculations. Up to 50% of chromium was predicted to be present as stable aqueous ions [dominated by $Cr(NH_3)_2(OH)_2^+$ cations] in the chromium chloride solution, while CrOOH was found to be the dominant solid form (50%). In contrast, less than 1% of nickel and cobalt ions were found to form aqueous ions in the solutions of nickel sulfate [dominated by $Ni\text{-}(COOH)_2$ ions] and cobalt chloride [dominated by $Co(NH_3)Cl^{2+}$], respectively. In the cocktail of all three salts, predicted

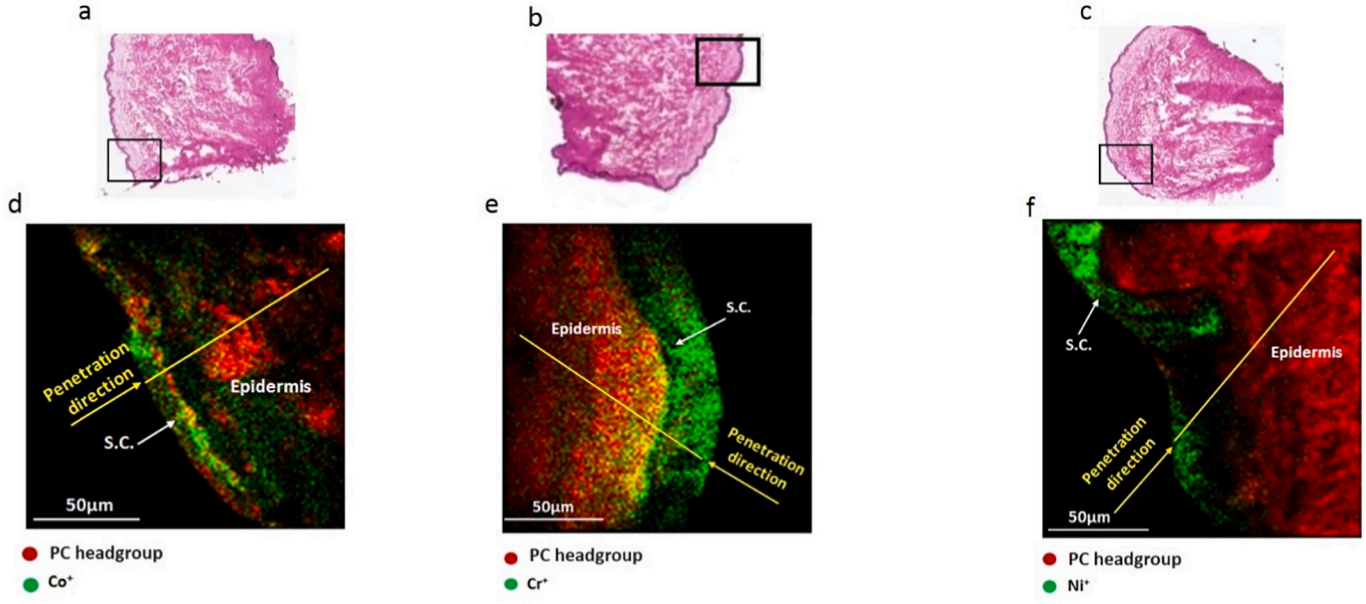

Fig. 1. H&E stained images of skin tissue sections exposed to a) cobalt chloride b) chromium chloride and c) nickel sulfate. The marked regions indicate the areas analyzed with ToF-SIMS. Red/green color overlay of ToF-SIMS ion images on the marked regions at a field of view of approximately 150 × 150 μm from skin tissue samples exposed to d) cobalt chloride e) chromium chloride and f) nickel sulfate showing Phosphatidylcholine (PC) headgroup signals in red and metal signals in green in each image. (For interpretation of the references to color in this figure legend, the reader is referred to the web version of this article.)

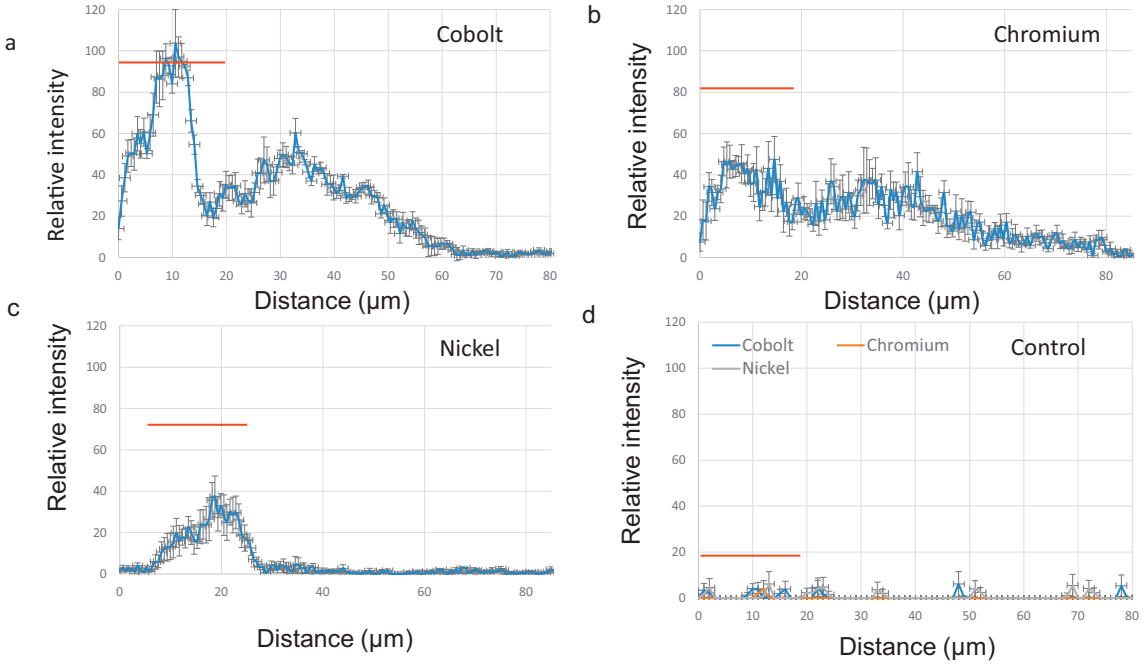

Fig. 2. Line scan analysis of ToF-SIMS ion images of skin tissue sections exposed to solutions of cobalt chloride, chromium chloride, and nickel sulfate respectively, showing the ion intensity of a) cobalt, b) chromium and c) nickel ions versus distance from the skin surface. d) shows cobalt, chromium and nickel distribution in the control. Stratum corneum layer thickness (approx. 20 μm) is marked with a red line along the x-axes. Each line scan is composed of an average of 4 individual line scans as can be seen in supplementary Fig. S4. Error bars are standard error of the mean. Cobalt and chromium ions penetrate into the skin tissue while nickel ions show the highest accumulation in the stratum corneum itself. (For interpretation of the references to color in this figure legend, the reader is referred to the web version of this article.)

soluble ions were dominated by chromium [$Cr(NH_3)_2(OH)_2^+$], while nickel and cobalt were almost entirely present in solid forms, most likely as nanoparticles of $Ni(OH)_2$ and Co_3O_4. These were also the predominant solid species in the single solutions of nickel and cobalt. No visible precipitation was observed in any of the solutions during the experiments. In the mixture, the concentration of aqueous chromium ions was approximately equal to that of the single chromium solution, however, the concentration of aqueous cobalt and nickel was more than two-fold lower as compared to their corresponding single solutions.

Metal haptens are small ions which can traverse through the primary barrier components and distribute further down through the epidermis. Their skin transport is determined by the size of metal ions, complexes, or nanoparticles, their charge, and their protein binding capacity. Chemical speciation modelling predicts equilibrium species and cannot give an answer on how rapidly this equilibrium is obtained. There could hence be a difference in time of reaching the equilibrium between the two metals that were predicted to be present predominantly in insoluble form (nickel and cobalt). The predicted soluble forms of nickel and cobalt differed in their charge, with the two times positively charged cobalt ion $Co(NH_3)Cl^{2+}$ being smaller in size than the neutrally charged nickel ion $Ni\text{-}(COOH)_2$, which hence could be an explanation for the higher skin penetration of cobalt as compared to nickel.

This study also confirms the findings of our previous work where nickel ions were found to accumulate mainly in the stratum corneum and to some extent in the upper parts of the epidermis(Malmberg et al., 2018). Similarly, in both individual and cocktail exposure experiments, nickel ions are found to be located almost entirely in the stratum corneum with little further penetration into the epidermis. The results are well correlated with previous results obtained from the scanning electron microscopy study by Kalimo et al. (Kalimo et al., 1985) where a heavy accumulation of nickel ions was found in the stratum corneum and very superficial locations of the epidermis in biopsies from patients exposed to nickel via patch testing. The same trend was seen in the tape stripping study by Hostynek et al. (Hostynek, 2003).

Our findings indicate that under these conditions, cobalt, and chromium (III) species penetrate considerably into the epidermis unlike nickel, as illustrated in Figs. 1 and 2. This is again in line with previous studies, where Cr (III) has been detected in the epidermis in biopsies from exposed patients and in ex vivo experiments using diffusion cells (Gammelgaard et al., 1992; Liden and Lundberg, 1979; Van Lierde et al., 2006). However, these studies are performed using methods which do not enable detailed information on the distribution in the skin layers. There is to the best of our knowledge no experimental studies investigating skin penetration of cobalt in human skin. The present results are thus the first published on this subject. The results are in line with studies of skin penetration of cobalt in piglet skin, where the piglet skin was homogenized, analyzed and results compared to cobalt levels in the receptor fluid of the diffusion cell (Midander et al., 2020).

In skin samples treated with the cocktail of metal salts, both cobalt and chromium species were found to penetrate more evenly into the epidermis compared to nickel species. Cobalt species show further penetration into the skin compared to chromium species, but lower total concentration in the skin as compared to chromium species. We speculate that the observed differences between cobalt and chromium can be explained by *i*) a higher fraction of soluble and hence mobile ions of chromium in solution, as predicted by the chemical speciation analysis, and *ii*) a more rapid binding of the trivalent chromium ions to skin proteins as compared to divalent cobalt ions. The very high binding capacity to proteins of the trivalent chromium ions as compared to divalent cobalt and nickel ions is expected (Hedberg et al., 2019). Rapid binding to skin proteins could hence hinder further transport into the skin.

In line with this is the hypothesis that skin penetration might be negatively correlated with the sensitization potency of haptens, and that a stronger sensitizer would react more quickly and accumulate in the stratum corneum, while non sensitizers would penetrate further into the skin. This is supported in the chemistry, since sensitization requires the metal ion to bind to proteins, and a rapid binding to skin proteins in the

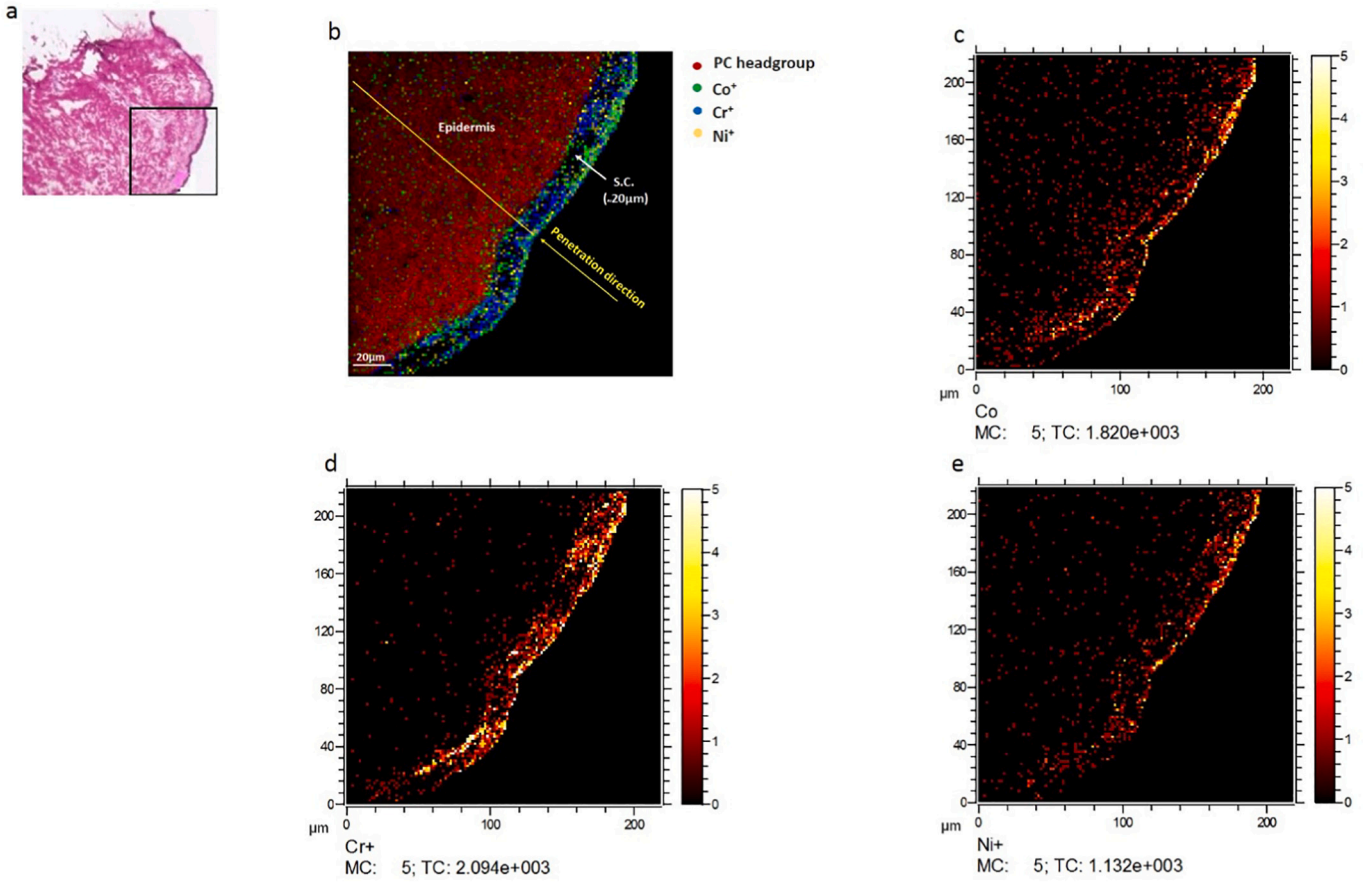

Fig. 3. a) H&E stained image of skin tissue exposed to a cocktail of nickel sulfate, cobalt chloride and chromium chloride. The marked region indicates the area analyzed with ToF-SIMS. b) Red/green/blue/yellow color overlay of ion image from ToF-SIMS analysis on the marked at a field of view of approximately 220 × 220 µm from skin tissue showing phosphatidylcholine (PC) headgroup signal in red, cobalt in green, chromium in blue and nickel in yellow. Single ion images used to create the RGB overlay in a of the skin penetration of c) cobalt d) chromium and e) nickel ions. (For interpretation of the references to color in this figure legend, the reader is referred to the web version of this article.)

stratum corneum could be caused by the same mechanism. This hypothesis has been supported by studies of fluorescent model haptens, showing that among structurally closely similar compounds, the compounds with higher sensitization potency are almost entirely localized to the stratum corneum (Samuelsson et al., 2009; Simonsson et al., 2012). Our observations show quite the opposite, where nickel, the weakest hapten, was found to be located mainly to the stratum corneum. In earlier studies of the sensitization potency of several metal salts including cobalt, chromium (VI) and nickel salts in mice, cobalt has the highest sensitizing potency and nickel the lowest (Basketter et al., 1999; Ikarashi et al., 1992). However, in cross reactivity studies in guinea pigs, chromium (III) was suggested as the main sensitizer and considered a stronger sensitizer than chromium (VI) (Siegenthaler et al., 1983). This stand in contrast to data from clinical investigations, where nickel by far is the most common cause of contact allergy in the general population (Thyssen et al., 2007). Nickel, cobalt and chromium are all present in everyday objects and exposure is frequent in general daily activities. As chromium and cobalt are stronger sensitizers, higher frequencies of contact allergy would be expected compared to that of nickel in the general population. However, many aspects influence the frequency of contact allergy to a compound in the population, such as skin exposure dose, skin penetration and sensitization potency of the compound. The high frequencies of contact allergy to nickel could be caused by a higher exposure to nickel compared to that of cobalt and chromium. It is also possible that the data from animal studies of sensitization potency of nickel are not directly applicable to humans, and that humans are more susceptible to nickel sensitization than mice (Schmidt et al., 2010). It is further possible that the chemical species of nickel formed in ion release from metal objects are different from those formed in the present study. This would indicate a further penetration of nickel species released from metal objects compared to the nickel species studied here. A higher sensitization potency in humans and a higher penetration of nickel from everyday metal objects compared to studied nickel salts could explain the high prevalence of contact allergy to nickel. However, nickel sulfate is the main salt used in patch testing for diagnosis of contact allergy to nickel and has been proved to detect clinically relevant nickel contact allergy (Thyssen et al., 2007). In the study by Kalimo et al., positive contact allergic skin reactions to nickel sulfate were biopsied and analyzed. Nickel was detected almost exclusively in the stratum corneum (Kalimo et al., 1985). This could indicate that the mechanism of skin penetration, as the first step of sensitization in contact allergy is more complex than previously thought.

In the study of skin penetration of the metal haptens present in the same cocktail, cobalt and chromium showed lower penetration into the skin tissue compared to the experiments with exposure to a single metal hapten. For cobalt, this is assumed to be due to the lower fraction of aqueous cobalt ions, as predicted from chemical speciation. Also, the coexistence of several metal ions at once could have accelerated the protein binding (Hedberg et al., 2019) and hence hindered further penetration. The reduction in penetration, could further be caused by a matrix effect, a common issue in ToF-SIMS in which signal intensity of species is possibly influenced by other species coexisting in the analysis environment (Nakano et al., 2018; Seah and Shard, 2018). However, such an effect is unlikely in this setup since the major matrix influence is

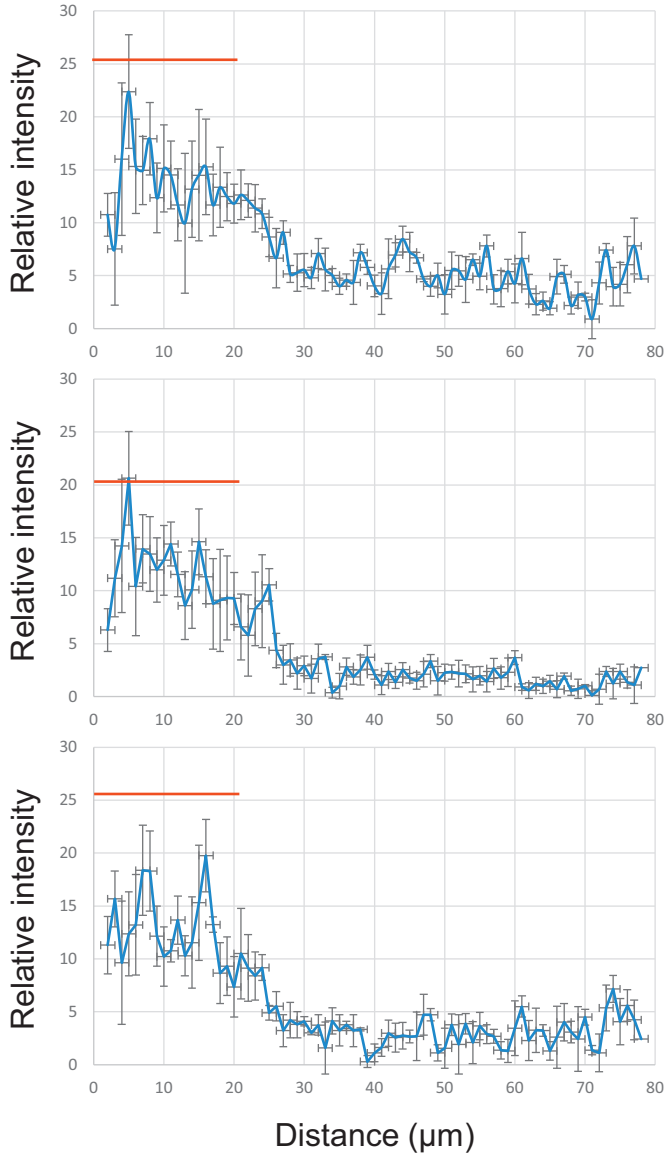

Fig. 4. Line scan analysis of ToF-SIMS ion images of skin tissue sections exposed to a solution of cobalt chloride, chromium chloride, and nickel sulfate in cocktail, showing the ion intensity of a) cobalt, b) chromium and c) nickel ions versus distance from the skin surface. Stratum corneum layer thickness (approx. 20 µm) is marked with a red line along the x-axes. Each line scan is composed of an average of 4 individual line scans (shown in supplementary Fig. S4d). Error bars are standard error of the mean. Chromium ions showed the strongest signal in the stratum corneum whereas cobalt was shown to penetrate deepest into the skin. The nickel ions accumulated in the stratum corneum with little penetration further into the skin. Generally, signals were weaker than in the experiments with single exposure. (For interpretation of the references to color in this figure legend, the reader is referred to the web version of this article.)

caused by the skin itself, which remains the same in all the experiments performed here. Our results are partly in contrast to an ICP-MS study showing that combined exposure to nickel, cobalt, and chromium caused a relatively higher retention of metals in piglet skin than exposure to the single metal ions (Midander et al., 2020). However, that study only examined exposure after 2 h in contrast to our 24 h exposure which could explain the apparent difference.

Our findings demonstrate that metal haptens mainly accumulated in the stratum corneum, but all three metal sensitizers could also be detected in the epidermis. Our method provided permeation profiles in skin for known sensitizers, on a level of detail not previously published. Imaging data of the distribution of cobalt ions in human skin is presented for the first time. The findings show that the permeation profiles are different, despite these sensitizers being all metal ions and common causes of contact allergy. Studying skin uptake by only considering penetration through the skin might therefore not give accurate results.

Funding source

The Swedish Skin Foundation and the WM Lundgren Research Foundation.

Declaration of Competing Interest

The authors declare that they have no known competing financial interests or personal relationships that could have appeared to influence the work reported in this paper.

Acknowledgements

Funding from the Swedish Skin Foundation, Stiftelsen Forska utan Djurförsök and from WM Lundgrens Research Foundation is gratefully acknowledged.

Appendix A. Supplementary data

Supplementary data to this article can be found online at https://doi.org/10.1016/j.tiv.2021.105232.

References

Basketter, D.A., Lea, L.J., Cooper, K.J., Ryan, C.A., Gerberick, G.F., Dearman, R.J., Kimber, I., 1999. Identification of metal allergens in the local lymph node assay. Am. J. Contact Dermat 10, 207–212.

Crosera, M., Adami, G., Mauro, M., Bovenzi, M., Baracchini, E., Larese Filon, F., 2016. In vitro dermal penetration of nickel nanoparticles. Chemosphere 145, 301–306.

Diepgen, T.L., Ofenloch, R.F., Bruze, M., Bertuccio, P., Cazzaniga, S., Coenraads, P.J., Elsner, P., Goncalo, M., Svensson, A., Naldi, L., 2016. Prevalence of contact allergy in the general population in different European regions. Br. J. Dermatol. 174, 319–329.

Filon, F.L., D'Agostin, F., Crosera, M., Adami, G., Bovenzi, M., Maina, G., 2009. In vitro absorption of metal powders through intact and damaged human skin. Toxicol. in Vitro 23, 574–579.

Gammelgaard, B., Fullerton, A., Avnstorp, C., Menne, T., 1992. Permeation of chromium salts through human skin in vitro. Contact Dermatitis 27, 302–310.

Hedberg, Y.S., Liden, C., 2016. Chromium(III) and chromium(VI) release from leather during 8 months of simulated use. Contact Dermatitis 75, 82–88.

Hedberg, Y.S., Erfani, B., Matura, M., Liden, C., 2018. Chromium(III) release from chromium-tanned leather elicits allergic contact dermatitis: a use test study. Contact Dermatitis 78, 307–314.

Hedberg, Y.S., Dobryden, I., Chaudhary, H., Wei, Z., Claesson, P.M., Lendel, C., 2019. Synergistic effects of metal-induced aggregation of human serum albumin. Colloids Surf. B: Biointerfaces 173, 751–758.

Hostynek, J.J., 2003. Factors determining percutaneous metal absorption. Food Chem. Toxicol. 41, 327–345.

Ikarashi, Y., Tsuchiya, T., Nakamura, A., 1992. Detection of contact sensitivity of metal salts using the murine local lymph node assay. Toxicol. Lett. 62, 53–61.

Kalimo, K., Lammintausta, K., Maki, J., Teuho, J., Jansen, C.T., 1985. Nickel penetration in allergic individuals: bioavailability versus X-ray microanalysis detection. Contact Dermatitis 12, 255–257.

Karlberg, A.T., Bergstrom, M.A., Borje, A., Luthman, K., Nilsson, J.L.G., 2008. Allergic contact dermatitis-formation, structural requirements, and reactivity of skin sensitizers. Chem. Res. Toxicol. 21, 53–69.

Lagrelius, M., Wahlgren, C.F., Matura, M., Kull, I., Liden, C., 2016. High prevalence of contact allergy in adolescence: results from the population-based BAMSE birth cohort. Contact Dermatitis 74, 44–51.

Larese Filon, F., Crosera, M., Timeus, E., Adami, G., Bovenzi, M., Ponti, J., Maina, G., 2013. Human skin penetration of cobalt nanoparticles through intact and damaged skin. Toxicol. in Vitro 27, 121–127.

Liden, S., Lundberg, E., 1979. Penetration of chromium in intact human skin in vivo. J. Investig. Dermatol. 72, 42–45.

Malmberg, P., Guttenberg, T., Ericson, M.B., Hagvall, L., 2018. Imaging mass spectrometry for novel insights into contact allergy - a proof-of-concept study on nickel. Contact Dermatitis 78, 109–116.

Midander, K., Schenk, L., Julander, A., 2020. A novel approach to monitor skin permeation of metals in vitro. Regul. Toxicol. Pharmacol. 115, 104693.

Nakano, S., Yamagishi, T., Aoyagi, S., Portz, A., Durr, M., Iwai, H., Kawashima, T., 2018. Evaluation of matrix effects on TOF-SIMS data of leu-enkephalin and 1,2-dioleoyl-sn-glycero-3-phosphocholine mixed samples. Biointerphases 13, 03B403.
Samuelsson, K., Simonsson, C., Jonsson, C.A., Westman, G., Ericson, M.B., Karlberg, A.T., 2009. Accumulation of FITC near stratum corneum-visualizing epidermal distribution of a strong sensitizer using two-photon microscopy. Contact Dermatitis 61, 91–100.
Schmidt, M., Raghavan, B., Muller, V., Vogl, T., Fejer, G., Tchaptchet, S., Keck, S., Kalis, C., Nielsen, P.J., Galanos, C., Roth, J., Skerra, A., Martin, S.F., Freudenberg, M. A., Goebeler, M., 2010. Crucial role for human Toll-like receptor 4 in the development of contact allergy to nickel. Nat. Immunol. 11, 814–819.
Seah, M.P., Shard, A.G., 2018. The matrix effect in secondary ion mass spectrometry. Appl. Surf. Sci. 439, 605–611.
Siegenthaler, U., Laine, A., Polak, L., 1983. Studies on contact sensitivity to chromium in the guinea pig. The role of valence in the formation of the antigenic determinant. J. Investig. Dermatol. 80, 44–47.
Simonsson, C., Stenfeldt, A.L., Karlberg, A.T., Ericson, M.B., Jonsson, C.A., 2012. The pilosebaceous unit—a phthalate-induced pathway to skin sensitization. Toxicol. Appl. Pharmacol. 264, 114–120.
Stefaniak, A.B., Duling, M.G., Geer, L., Virji, M.A., 2014. Dissolution of the metal sensitizers Ni, Be, Cr in artificial sweat to improve estimates of dermal bioaccessibility. Environ Sci Process Impacts 16, 341–351.
Tanojo, H., Hostynek, J.J., Mountford, H.S., Maibach, H.I., 2001. In vitro permeation of nickel salts through human stratum corneum. Acta Derm. Venereol. Suppl. 19–23.
Thyssen, J.P., Menne, T., 2010. Metal allergy–a review on exposures, penetration, genetics, prevalence, and clinical implications. Chem. Res. Toxicol. 23, 309–318.
Thyssen, J.P., Linneberg, A., Menne, T., Johansen, J.D., 2007. The epidemiology of contact allergy in the general population - prevalence and main findings. Contact Dermatitis 57, 287–299.
Thyssen, J.P., Gawkrodger, D.J., White, I.R., Julander, A., Menne, T., Liden, C., 2013. Coin exposure may cause allergic nickel dermatitis: a review. Contact Dermatitis 68, 3–14.
Van Lierde, V., Chery, C.C., Roche, N., Monstrey, S., Moens, L., Vanhaecke, F., 2006. In vitro permeation of chromium species through porcine and human skin as determined by capillary electrophoresis-inductively coupled plasma-sector field mass spectrometry. Anal. Bioanal. Chem. 384, 378–384.
Vanbellingen, Q.P., Elie, N., Eller, M.J., Della-Negra, S., Touboul, D., Brunelle, A., 2015. Time-of-flight secondary ion mass spectrometry imaging of biological samples with delayed extraction for high mass and high spatial resolutions. Rapid Commun. Mass Spectrom. 29, 1187–1195.